AIAA SciTech Forum
8-12 January 2024, Orlando, FL
AIAA SCITECH 2024 Forum

10.2514/6.2024-0484

Evaluation of a Planar Scandate Cathode for Hall Thruster Operation

Allison E. Timm* and Joshua L. Rovey †
University of Illinois Urbana-Champaign, Urbana, Illinois, 61801

Bernard Vancil‡
e beam, inc., Beaverton, Oregon, 91070

Cathodes are often implemented as a component of electrostatic electric propulsion devices to enable plasma production and to minimize spacecraft charging. However, cathodes can be a limiting factor on the lifetime and operation of thrusters due to eventual degradation of the emitting surface. This study evaluated the operational characteristics and plasma plume properties of a planar scandate cathode to assess the feasibility of the cathode supporting operation of a Hall effect thruster. The cathode was operated in a pure xenon environment within a sealed vacuum tube. Two operational modes were studied: cup connected and cup disconnected. In each mode, the cathode was operated at a series of heater voltages and anode currents to investigate operational behavior. Analysis of the cup disconnected data produced plasma plume properties including the electron current, electron current density, electron density, plasma density, and electron temperature. The cathode produced a maximum electron current of 3 A, a maximum electron current density of 616 $\frac{A}{cm^2}$ at the cup orifice, an average electron density and plasma density on the order of 10^{13} cm^{-3}, and an electron temperature ranging from 0.53 eV to 0.87 eV. These plasma properties are comparable to the plasma plume properties generated by hollow cathodes that have successfully operated with a Hall effect thruster. The planar scandate cathode has been shown to produce 3 A of electron current which suggests that it may operate any Hall thruster that requires a discharge current of up to 3 A. Since the planar scandate cathode produces plasma properties that are comparable to existing cathodes and sufficient electron current to operate a Hall thruster, it is reasonable to conclude that the cathode should be considered as a candidate for Hall thruster operation.

I. Introduction

Cathodes are electron emission devices that are typically implemented alongside electrostatic electric propulsion (EP) plasma devices. These devices include ion thrusters and Hall effect thrusters which require the presence of electrons for ionization of the propellant gas and neutralization of the plasma plume. Ionization of the propellant allows for the production of a plasma discharge while neutralization of the plume mitigates spacecraft charging [1].

The primary cathode geometry used in electric propulsion is the hollow cathode. Hollow cathodes are comprised of five main components: heater, cathode tube, cathode insert, orifice, and keeper. A schematic of a typical hollow cathode is shown in Fig. 1. The propellant gas is first introduced into the cathode insert region surrounded by the cathode tube. This is known as the emitter region and is responsible for the excitation of the working gas, emission of electrons, and generation of a dense plasma. Once a dense plasma is formed in the emitter region, the plasma proceeds to the orifice which is a region of high current density [1, 2]. The orifice increases the pressure in the cathode insert region to maintain the dense internal plasma. The plasma heats the insert region to the temperature required for reliable cathode electron emission [3]. The emission temperature is dependent on the material composition of the emitting surface and its work function. Following the orifice, the keeper applies an electric field to the internal plasma forming a plasma discharge, or plasma plume, as seen in Fig. 1. This region of the cathode sustains a diffuse plasma which connects to the thruster discharge plasma as well as neutralizes the thruster beam [1, 2].

*National Defense Science and Engineering Graduate Research Fellow, Department of Aerospace Engineering, AIAA Student Member. aetimm2@illinois.edu
†Professor, Department of Aerospace Engineering, AIAA Associate Fellow. rovey@illinois.edu
‡President. bernie@ebeaminc.com

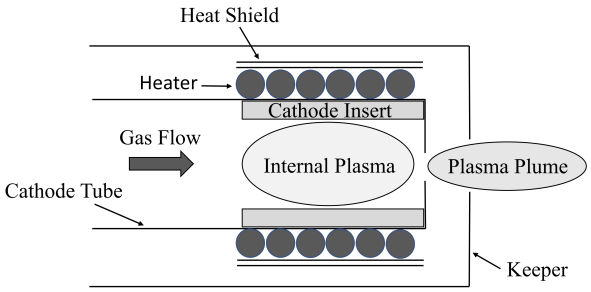

Fig. 1 Hollow Cathode Geometry

An alternative cathode geometry that could be implemented in electrostatic EP systems is a planar cathode as shown in Fig. 2. The planar cathode assembly includes an electrical feedthrough, propellant feedthrough, orifice cup, heater, planar cathode, and keeper. The propellant gas is introduced into the center of the cathode assembly, which is surrounded by the rear assembly and the orifice cup, through the propellant feedthrough. The orifice cup is present to create a high pressure region in which breakdown can easily occur. In hollow cathodes, the high pressure region exists because the propellant is flown through a hollow emitter structure that has an orifice at the exit. Planar cathodes require the introduction of an orifice cup to produce a similar high pressure region allowing for breakdown. The planar cathode insert is mounted on a resistive heater which is responsible for heating the cathode to emission temperature, outgassing any contaminants adsorbed to the cathode surface, and regenerating the cathode emitting surface. A dense plasma is generated inside of the orifice cup as shown in Fig. 2. Similar to the hollow cathode, the keeper applies an electric field to the internal plasma leading to the generation of a plasma plume through the orifice. This plasma connects to the thruster plasma as well as neutralizes the thruster beam.

The most widely implemented cathode material is barium (Ba). Barium cathode inserts are manufactured by impregnating tungsten with barium. As the cathode temperature increases, barium is released and moves through the tungsten to the surface where it creates a barium monolayer. The monolayer is a low work function emitting surface with a work function of around 2.7 eV [4]. The low work function surface emits the electrons required for plasma production. Over time, the barium depletes which decreases the rate at which barium is introduced into the monolayer. This leads to an increase in the work function of the emitting surface and eventually affects cathode lifetime due to insufficient production of the electrons required to ignite or sustain a plasma [3, 5, 6]. Prior to degradation, barium cathodes typically produce a current density of 1 to 10 A/cm^2 [1]. Barium cathodes can also become poisoned over time due to the development of an oxide layer either from being exposed to the atmosphere or by operating with an oxygen contaminated propellant. Poisoning will occur if the propellant has an oxygen partial pressure that exceeds 10^{-6} Torr [7]. Previous studies have attempted to mitigate cathode poisoning by using LaB_6 (lanthanum hexaboride) for the insert material instead of barium [8–10].

An alternative cathode material is scandium oxide (Sc_2O_3), also known as scandate. Scandate cathode inserts are manufactured by impregnating tungsten with scandium oxide. As the cathode heats, the scandium is transported to the surface of the insert where it creates a semi-conducting layer along with barium and oxygen. This layer operates similarly to the barium cathode by creating a low work function emitting surface, with a work function of around 1.5 eV, that produces the electrons sufficient to support plasma generation [11]. However, unlike the barium cathode, the scandium does not deplete which increases the lifetime of the cathode and subsequently the thruster. Additionally, this type of cathode insert produces current densities greater than 10 A/cm^2. Scandate cathodes can also be reactivated if they are no longer producing electrons at the rate required for operation. Insufficient emission can be a bi-product of electrical arcing to the cathode surface. Arcing can cause the low work function scandium surface to be knocked off, thereby decreasing the electron emission capability. The reactivation process involves heating the cathode for a period of two hours to two days to bring a new layer of scandium oxide up to the surface of the cathode. The regenerative nature of scandate cathodes makes them more robust than barium cathodes [12–14].

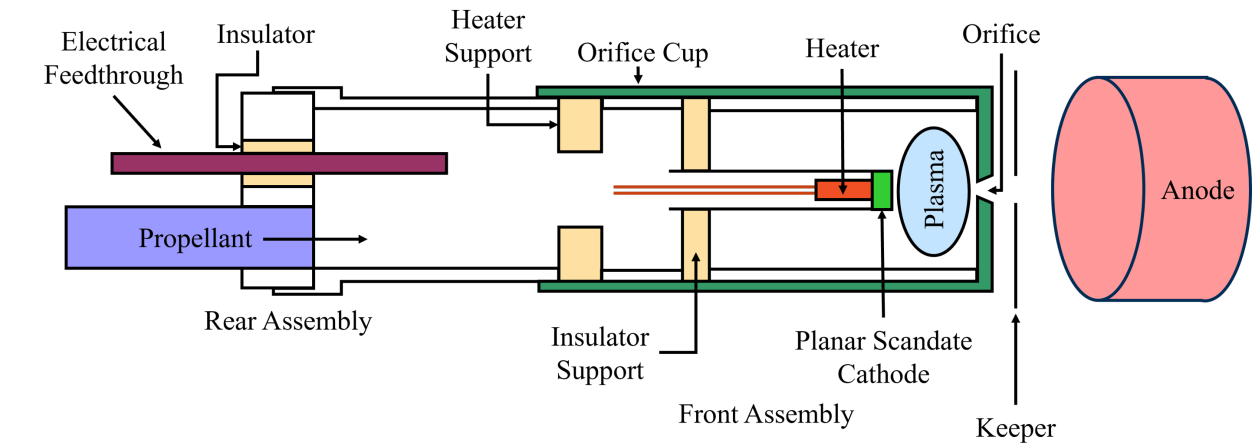

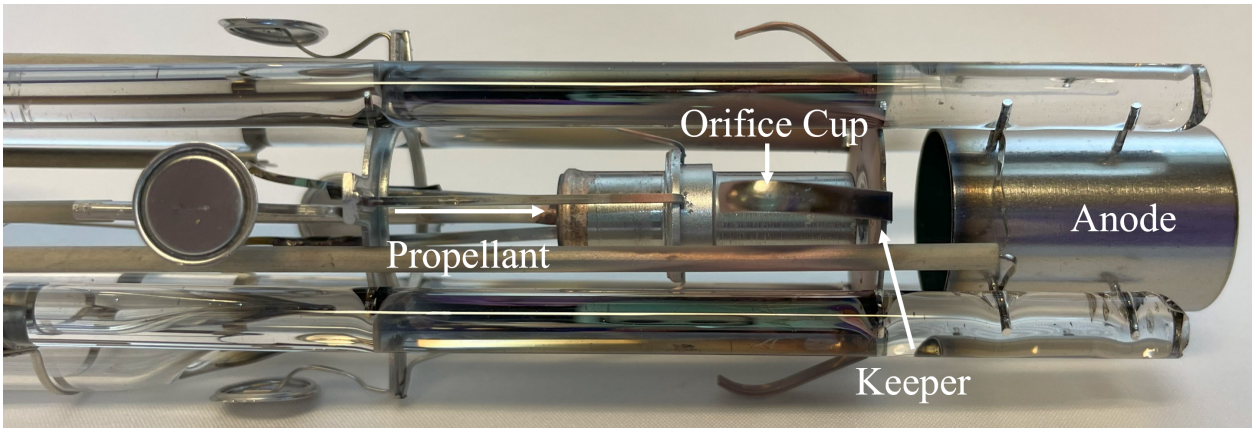

Fig. 2 Planar cathode diagram compared with cathode tube assembly. Schematic recreated from a diagram provided by e beam, inc.

There have been a range of studies evaluating the material properties of scandate cathodes and their subsequent electron emission capabilities [15–20]. These studies include emission characterization as well as demonstration of scandate cathode inserts in a hollow cathode geometry. Additionally, an investigation into the implementation of scandate cathode inserts in a planar cathode geometry was conducted by Ohlinger [21]. While this investigation demonstrated the benefits of scaling cathode technology for low power electric propulsion applications, there was no conclusive evidence presented to suggest that the cathode would be suitable for implementation in an electrostatic electric propulsion configuration.

The objective of this investigation was to evaluate the operational characteristics of a planar scandate cathode and associated plasma plume properties to determine the feasibility of the cathode supporting operation of a Hall effect thruster. The remainder of this paper is organized as follows: Section II will describe the methodology, experimental setup, testing procedure, and data analysis technique used to evaluate the cathode. Section III will present the cathode evaluation results as well as further analysis to demonstrate the cathode's viability for implementation in a Hall thruster configuration. The paper will be concluded in Section IV.

II. Methodology

The planar scandate cathode evaluated in this study was the e beam, inc. planar scandate cathode shown in Fig. 3. The cathode assembly contained all of the components shown previously in Fig. 2. Following manufacturing, the cathode assembly and anode were enclosed in a glass tube and put under vacuum. Once under vacuum, a small quantity of xenon was introduced into the tube. The tube is a pure xenon self-contained testing configuration with a background pressure greater than 10^{-3} Torr. The background xenon gas serves as the propellant gas for the cathode plasma discharge.

Fig. 3 e beam, inc. planar scandate cathode tube

A. Cathode Operation

Prior to cathode ignition, the scandate insert was heated to electron emission temperature by applying 7.5 V to the resistive heater. During cathode ignition, the anode was biased to 70 V with a current limit of 3 A and the keeper was biased to 300 V with a current limit of 1 A. This initiated breakdown inside of the orifice cup and resulted in the formation of a plasma plume through the cup orifice. Following cathode ignition, the keeper was turned off and consistent plasma production was driven by the barrel anode. The anode is the rightmost cylinder downstream of the orifice cup and the keeper as shown in Fig. 2. Once the cathode was emitting electrons and producing a plasma, the heater was not necessarily required to maintain cathode temperature. If there is sufficient ion bombardment on the cathode surface, the heater can be turned off and the cathode will continue emitting electrons.

The cathode can operate in two different modes: cup connected and cup disconnected. In cup connected mode, the cup was shorted to the planar cathode. In cup disconnected mode, the cup floated independent of the planar cathode. When the orifice cup is shorted to the planar cathode, current flows from the anode to both the cup and the cathode. Since both the cup and the cathode are receiving current, the cathode operates at a lower temperature because it is not accepting all of the anode current. The lower operational temperature of the cathode increases the lifetime of the cathode [22]. When the orifice cup is floating independent of the cathode, current only flows from the anode to the cathode. This causes the cathode to operate at a higher temperature which can eventually put a limit on lifetime.

The two main parameters that affect cathode performance are heater voltage and anode current. In this study, the anode was operated in current controlled mode and the heater was operated over a range of voltages. The cathode was evaluated in both cup connected and cup disconnected configurations. In each configuration, the cathode was operated over a series of heater voltages: 0 V, 2 V, 4 V, and 6 V. At each heater voltage, the anode current was swept from 1 A to 3 A in increments of 0.2 A every minute. Measurements were taken at each current level to examine cathode behavior. In cup connected mode the anode power supply voltage, anode current, cathode current, and cup current were measured. In cup disconnected mode the anode power supply voltage, anode current, cathode current, and cup voltage were measured. The same data set was collected at t + 0 hours and t + 24 hours to determine if there was any appreciable difference in operation based on the duration of operation.

B. Measurement Circuit

The measurement circuit used to evaluate the cathode is shown in Fig. 4. The circuit includes the anode power supply and a voltage divider to measure the anode power supply voltage. The circuit also includes a series of resistors to

measure the anode current, cup current or voltage, and cathode current. The anode power supply voltage was measured using the voltage divider measurement resistor labeled Anode PS Voltage. The anode power supply voltage was measured by documenting the differential voltage across the measurement resistor. This differential voltage was read by an NI USB-6210 Data Acquisition System (DAQ) and loaded into a LabView VI that converted the differential voltage across the resistor to the anode power supply voltage. The anode current was measured by documenting the differential voltage across a resistor that was passed through an amc1300 precision isolation amplifier and was read by the DAQ into the LabView VI. The differential voltage was used along with the resistance value of 0.06 Ω to calculate the current flowing to the anode from the power supply. The current flowing to the anode, from the anode power supply, is the discharge current of the system. The discharge current passed from the anode through the plasma and into the cathode or the cathode and the cup depending on the operational mode. The cathode current was determined by measuring the differential voltage across the cathode resistor and dividing it by the 0.1 Ω resistor. The cup current was determined by measuring the differential voltage across the cup resistor and dividing it by the 0.1 Ω resistor in the cup connected mode. For the cup connected operational mode, all measurements were loaded into LabView. In cup disconnected mode, the cup was allowed to float independent of the cathode by opening the switch shown in Fig. 4. The only difference in the measurement circuit for the cup disconnected mode was that the cup resistor was disconnected from the DAQ in case the measured voltage exceeded the $\pm 10\ V$ voltage range limitation of the DAQ. Instead of using the DAQ, the positive terminal of a FLUKE 179 True RMS Multimeter was connected to the cup resistor and the negative terminal was connected to ground. The floating voltage was recorded at the end of each minute testing segment. The final thing to note about the measurement circuit is that the negative terminal of the anode power supply was grounded.

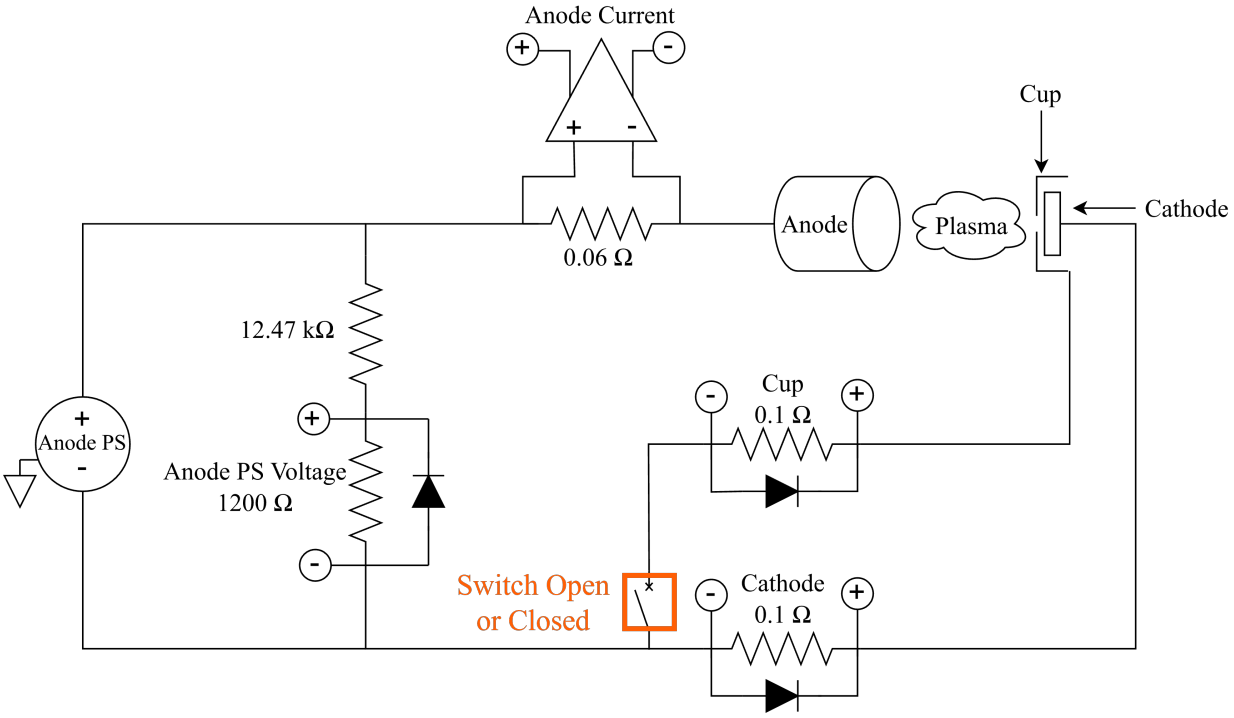

Fig. 4 Measurement circuit configuration

All measurements, except for the cup voltage, were recorded using the DAQ and LabView VI. For each heater voltage, data was collected for one minute at each anode current. The sampling rate of the VI was 1 kHz. Following data collection, the anode current, anode power supply voltage, cathode current, and cup current data were each averaged individually over the one minute segment at each anode current level. The standard deviation of each averaged section for each measurement quantity was used as the error in the measurement. The error in the cup voltage was the measurement error of the FLUKE 179 True RMS Multimeter. The anode power supply voltage was also adjusted by subtracting the voltage drop caused by the anode current measurement resistor to achieve the anode voltage. The data for each heater voltage, anode current, and cup configuration was used to produce I-V curves to assess cathode behavior. Further analysis, as laid out in the following sections, was conducted for the cup disconnected configuration.

C. Electron Current Analysis: Cup Disconnected

The anode current measured in this experiment was the electron current produced by the cathode [1]. In addition to the measured electron current, the cup has an orifice radius of 0.03937 cm (0.0155 inches). Based on the electron current and the orifice radius, the electron current density at the cup orifice can be calculated using Eq. 1.

$$J_e = \frac{I_e}{A} \tag{1}$$

Here, J_e is the electron current density, I_e is the electron current, and A is the area of the cup orifice. In addition to the electron current density, the electron density and plasma density can be determined. Inside of the cathode tube assembly, it was assumed that the electrons were stationary at the cathode and were accelerated across a differential voltage towards the anode. The cathode was grounded and the anode was biased to some potential. Applying conservation of energy, the electrons began with all potential energy at the cathode and only had kinetic energy at the anode. Based on this assumption, the electron velocity could be calculated using Eq. 2.

$$v = \sqrt{\frac{2eV}{m}} \tag{2}$$

In this expression, v is the velocity of an electron, e is the fundamental charge, V is the anode voltage, and m is the mass of an electron. The velocity of an electron depends on the current state of the anode voltage and thus does not remain constant over the duration of testing. The electron velocity was dependent on the operational conditions including the heater voltage and the anode current. Using the electron velocity, the electron density of the plasma can be calculated using Eq. 3.

$$I_e = n_e e v A \tag{3}$$

Here, n_e is the electron density and A is the area of the cup orifice [1]. Assuming that the plasma is quasi-neutral, where the electron density (n_e) is approximately equal to the ion density (n_i), the density of the plasma (n) can be calculated using Eq. 4.

$$n = n_e + n_i = 2 * n_e \tag{4}$$

D. Cup Floating Analysis: Cup Disconnected

In cup disconnected mode, the cup was floating independent of the cathode and the floating voltage of the cup was measured. The cup was an unbiased electrode present in the plasma and therefore its electric potential is equal to the plasma floating potential [23]. Based on this relationship, the electron temperature could be estimated using Eq. 5.

$$\frac{eV_f}{kT_e} = \frac{1}{2} ln \left(\frac{\pi}{2} \frac{m_e}{m_i} \right) \tag{5}$$

Here, V_f is the floating potential, k is the Boltzmann constant, T_e is the electron temperature in K, m_e is the mass of an electron, and m_i is the mass of the working gas (xenon, in this case) [24–26].

III. Results and Discussion

A. General Cathode Operation

As previously described, the cathode was operated in cup connected and cup disconnected modes. In each of these modes a set of measurements were taken for a range of anode currents and heater voltages. The data that were collected are presented in the following sections.

1. Cup Connected

The cathode was first evaluated in cup connected mode. The anode current and anode voltage at t + 0 hours and t + 24 hours is plotted in Fig. 5. Additional curves are shown for April 2023 and August 2023 for heater voltages of 6 V, 4 V, and 2 V (collected by e beam, inc.). The first notable characteristic of cathode operation is that the anode voltage increases by up to 2 V as the heater voltage decreases from 6 V to 0 V. As the heater voltage decreases, the cathode is no

longer emitting as readily because it is no longer being sufficiently heated by the heater. The anode voltage increases by up to 2 V to offset the heating deficit by increasing the temperature of the plasma and thereby keeping the cathode at a high enough temperature to efficiently emit electrons. Additionally, across the four data sets presented in Fig. 5, there is minimal variation, less than 2 V, in anode voltage due to duration of operation or when the measurements were taken. The anode voltage varies by a maximum of 2 V for any given heater voltage. This signifies relatively stable operation over time. Examination of the anode voltage at t + 0 and t + 24 hours reveals a decrease in anode voltage due to increased electron emission from the cathode surface after sustaining a plasma for a longer quantity of time.

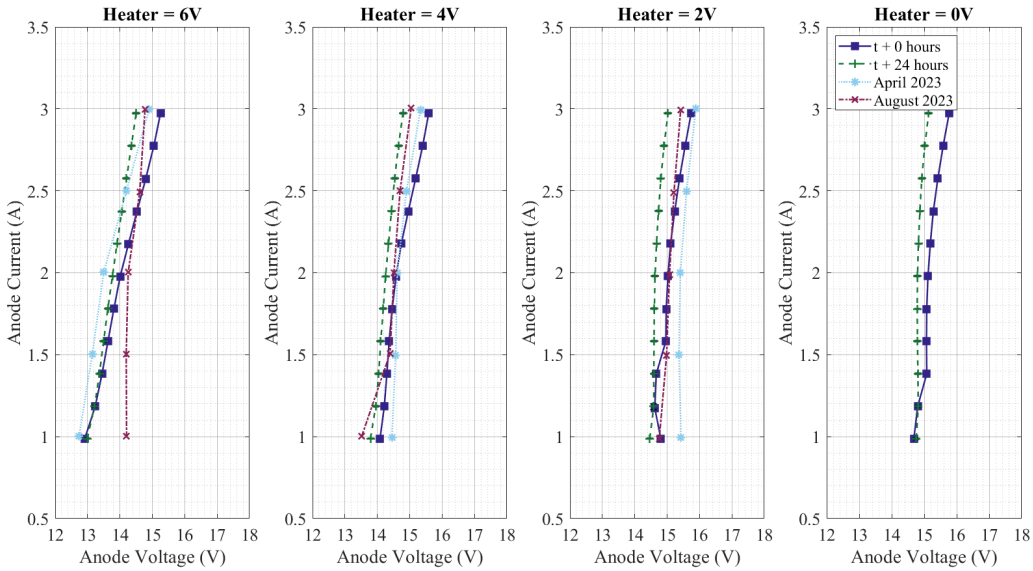

Fig. 5 Anode current with respect to anode voltage with the cup connected to the cathode. The data sets for t + 0 and t + 24 hours were taken in September 2023. The other two data sets were provided by e beam, inc. from previous testing.

The cathode current and anode voltage at t + 0 hours and t + 24 hours for the cup connected mode is shown in Fig. 6. The same variation in anode voltage is observed here due to the cathode emitting surface heating and emitting more readily after 24 hours of plasma operation and cathode heating. However, in cup connected mode, the cathode current remains mostly consistent, within 0.25 A, regardless of the duration of operation for any given heater voltage and anode voltage. The cathode receives a fraction of the anode current and the other portion is diverted to the cup.

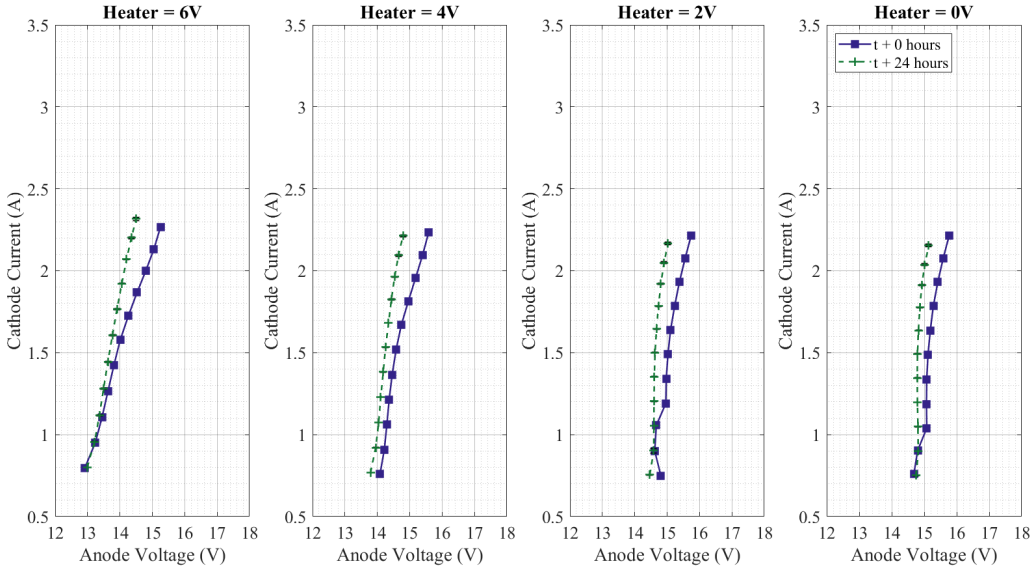

Fig. 6 Cathode current with respect to anode voltage with the cup connected to the cathode.

The cup current and anode voltage at t + 0 hours and t + 24 hours for the cup connected mode is shown in Fig. 7. The cup current accounts for the reminder of the anode current that does not flow to the cathode. The cup current increases, by up to 0.2 A, with decreasing heater voltage because the cathode is emitting fewer electrons due to lower insert temperatures. Therefore, the cup current increases to compensate for the decrease in cathode current. The cup current for any given heater voltage and anode voltage decreased, by at most 1 V, from t + 0 hours to t + 24 hours.

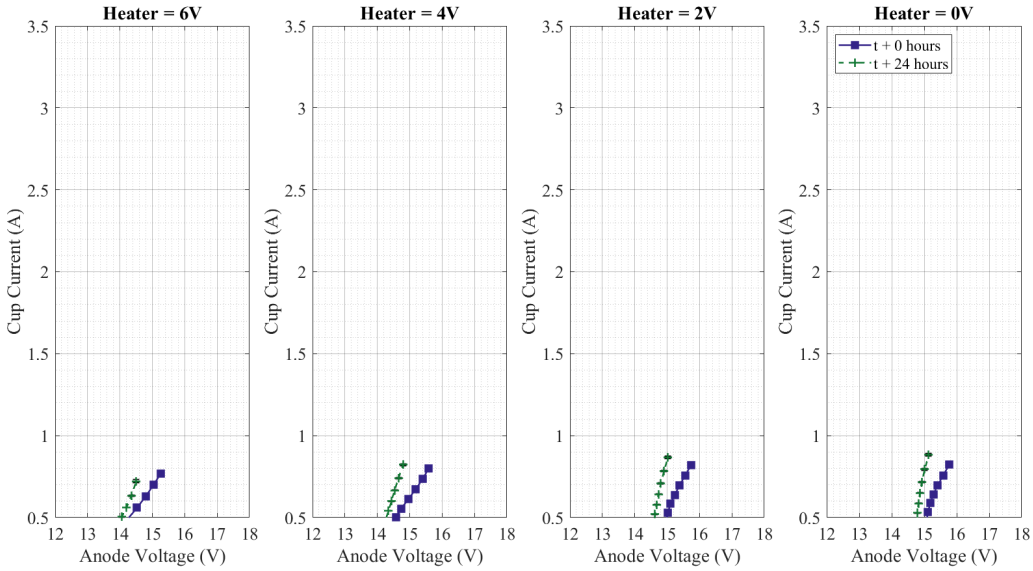

Fig. 7 Cup current with respect to anode voltage with the cup connected to the cathode.

2. Cup Disconnected

The cathode was also evaluated in cup disconnected mode. The anode current and anode voltage measured in this study at t + 0 and t + 24 hours is plotted in Fig. 8. As with the cup connected mode, the anode voltage increased by up

to 1.5 V as the heater voltage decreased, from 6 V to 0 V, to compensate for less cathode heating provided by the heater. In cup disconnected mode the anode voltage did not decrease from t + 0 hours to t + 24 hours. One possible reason for this is that in cup disconnected mode, the cup is a source of secondary electron emission which aids in cathode heating. This extra source of cathode heating minimizes the settling of anode voltage from t + 0 hours to t + 24 hours.

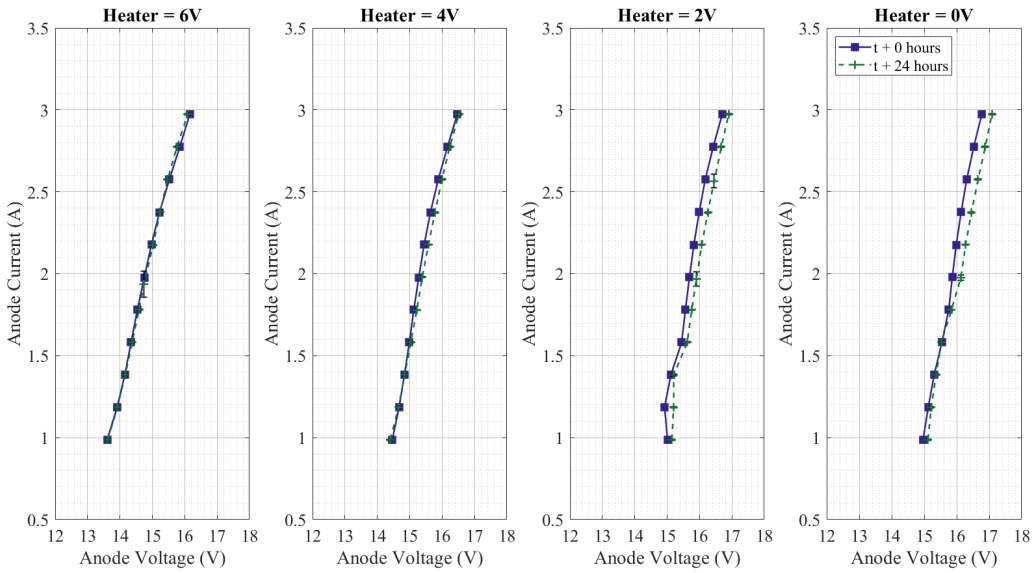

Fig. 8 Anode current with respect to anode voltage with the cup disconnected from the cathode.

The cathode current and anode voltage are plotted in Fig. 9. The cathode current plot, Fig. 9, and the previous anode current plot, Fig. 8, should be identical to each other because the anode current is driving the cathode plasma discharge. However, the cathode current measured by the circuit is on the order of 0.1 A higher than the anode current being fed into the system. One possible explanation for this phenomena is secondary emission due to the floating cup. The cup is undergoing ion bombardment which causes secondary emission. The secondary emission is in the vicinity of the cathode and could be causing more ions to bombard the surface of the cathode than were initiated by the anode. This could cause the cathode current to be higher than the current being introduced by the anode.

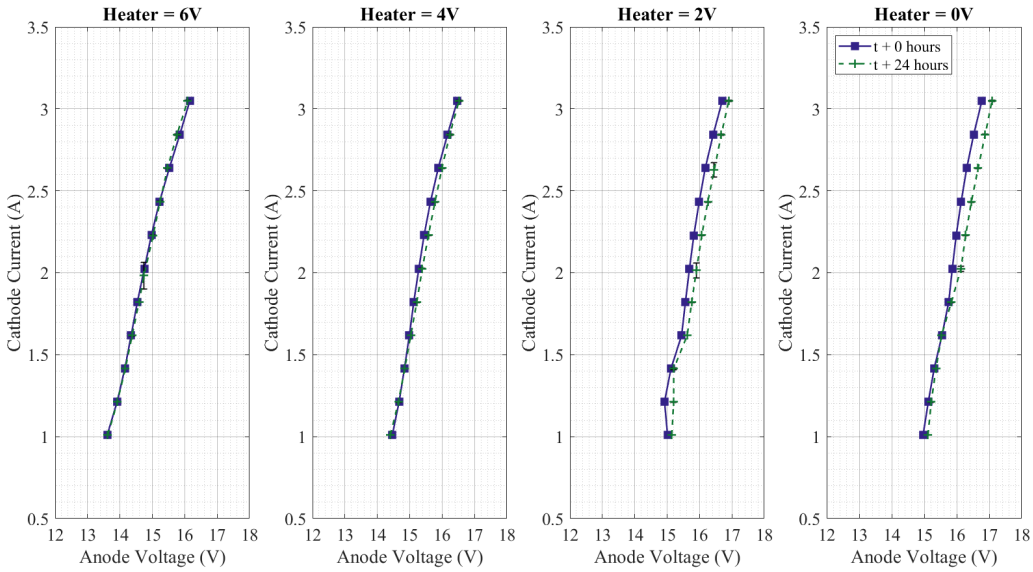

Fig. 9 Cathode current with respect to anode voltage with the cup disconnected from the cathode.

In cup disconnected mode, the ion and electron flux to the cup is equal, resulting in no net current to the cup. However, the cup voltage was measured and is plotted with respect to anode voltage at t + 0 hours and t + 24 hours in Fig. 10. The cup voltage is the floating potential of the plasma as detailed in Section II. Since the cup voltage is the floating potential of the plasma, the floating potential increases up to 2 V with an increase in anode voltage because there is more power driving the plasma. The floating potential of the plasma also increases with decreasing heater voltage because the cathode is no longer readily emitting electrons due to the external heat applied by the resistive heater. Based on this effect, the anode supplies more voltage to the plasma and the floating potential of the plasma increases. This maintains the operational temperature of the cathode as the heater voltage decreases.

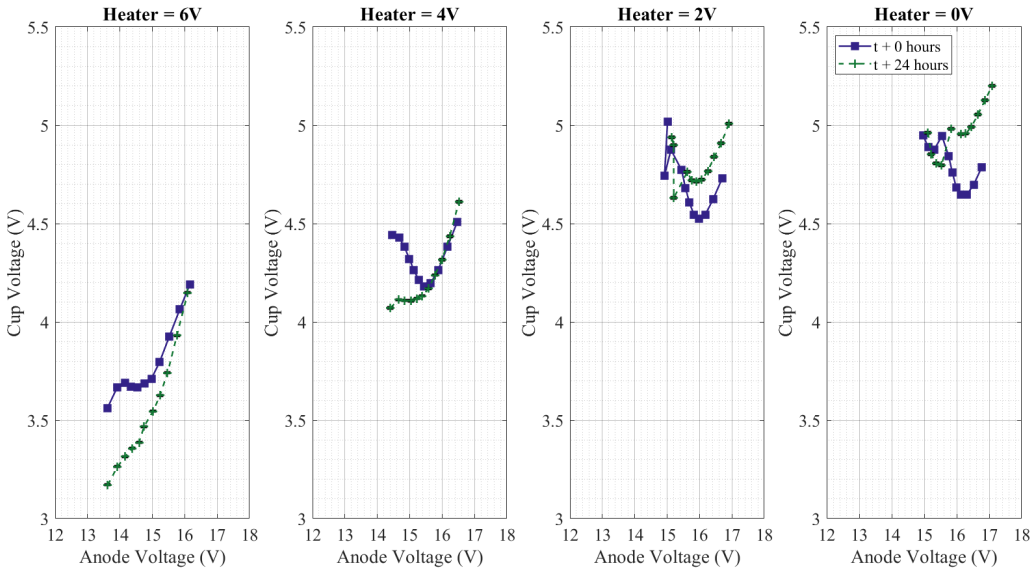

Fig. 10 Cup voltage with respect to anode voltage with the cup disconnected from the cathode.

B. Further Analysis for Hall Thruster Applicability

Further analysis of the cup disconnected mode was done to determine the viability of this cathode to be implemented in Hall thruster operation. In cup disconnected mode, all of the current is passed from the anode to the cathode. This is the discharge current or the electron current present in the system. The electron current (anode current in the figures) was swept from 1 A to 3 A. The electron current density at the cup orifice was calculated for an electron current of 1 A, 2 A, and 3 A and the results are shown in Table 1. The electron current densities exceeded that of a barium cathode by an order of magnitude and support the claim that scandate cathodes have an electron current density of at least 10 A/cm^2 [1, 12].

Table 1 Electron current and electron current density at the cup orifice

Electron Current (A)	Electron Current Density (A/cm^2)
1	205
2	411
3	616

Given the electron current, the electron density was determined utilizing Eq. 2 and 3. A plot of electron density with respect to anode current (electron current) is shown in Fig. 11. The electron density linearly increased with the electron current of the plasma. The electron density also decreases by up to 6% of the maximum with decreasing heater voltage because the cathode is emitting fewer electrons at lower heater voltages. This is due to the fact that the surface is not maintaining an optimal emission temperature. Based on this analysis, this cathode maintains an average electron density of $1.08 * 10^{13}\ cm^{-3}$. Assuming that the plasma was quasi-neutral, the average plasma density may be estimated as $2.16 * 10^{13}\ cm^{-3}$.

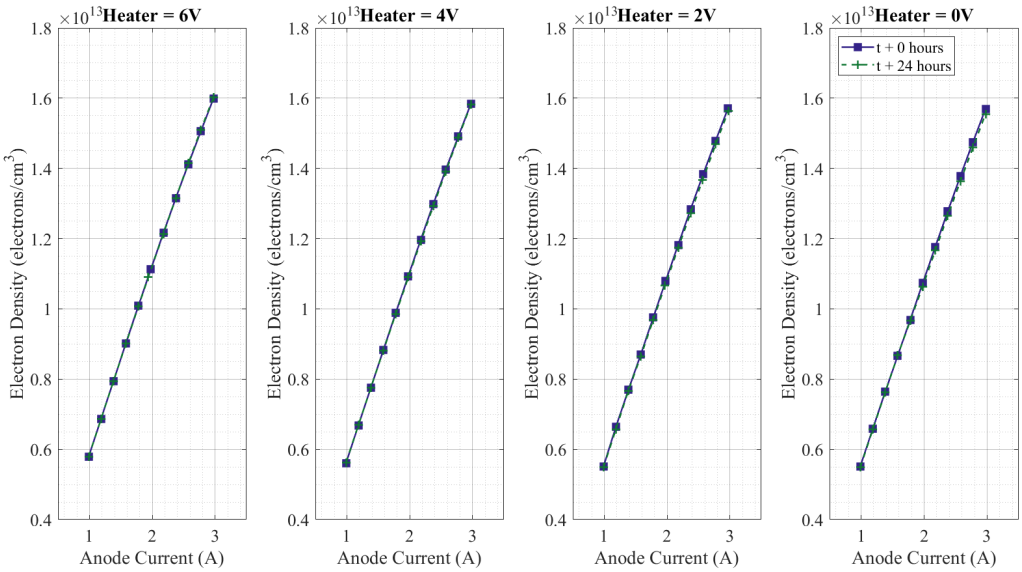

Fig. 11 Electron density with respect to anode (electron) current with the cup disconnected from the cathode.

The electron temperature was calculated using Eq. 5 for all heater voltages and anode currents. The resulting electron temperature plotted with respect to anode current (electron current) is shown in Fig. 12. The electron temperature increased by up to 0.25 eV with decreasing heater voltage because the plasma had to become more energetic in order to keep the cathode insert hot enough to sustain electron emission. The cathode generated a plasma with electron temperatures ranging from 0.53 eV to 0.87 eV.

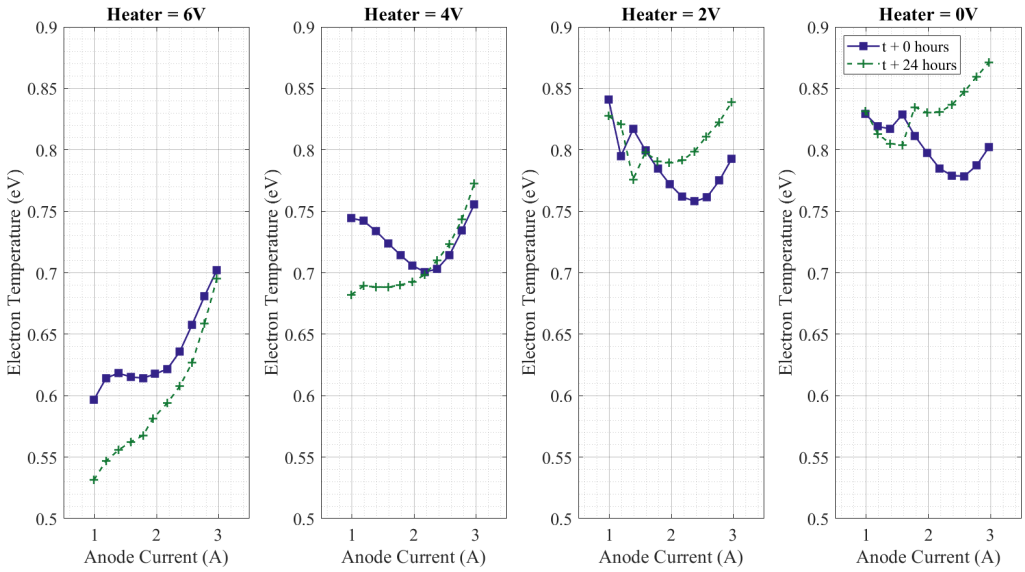

Fig. 12 Electron temperature with respect to anode (electron) current with the cup disconnected from the cathode.

C. Viability for Hall Thruster Implementation

Based on the above analysis, the cathode successfully produced and maintained a xenon plasma with properties as shown in Table 2. The cathode produced a maximum electron current of 3 A and a maximum electron current density of 616 $\frac{A}{cm^2}$. In addition, it produced an average electron density on the order of 10^{13} cm^{-3}, an average plasma density on the order of 10^{13} cm^{-3}, and an electron temperature ranging from 0.53 eV to 0.87 eV. The plasma properties measured in this study can be compared with those presented in existing experimental studies of hollow cathodes which enable Hall thruster operation. These hollow cathodes were evaluated in flowing xenon environments with a simple ring or planar anode downstream of the cathode. The list of cathodes, their relevant plasma properties, and applicable Hall thrusters is also presented in Table 2. The plasma properties include electron current (I_e), electron density (n_e), plasma density (n), and electron temperature (T_e).

Table 2 Comparison of the plasma properties of the planar scandate cathode and existing cathodes that successfully operate Hall thrusters [27].

Cathode	I_e (A)	n_e (cm^{-3})	n (cm^{-3})	T_e (eV)	Hall Thruster
Planar Scandate Cathode	3	10^{13}	10^{13}	0.53 - 0.87	—
BHC-2500	0.25	10^{11}	10^{11}	0.7	BHT-1500 [28]
SHC-M1	0.4 - 1.2	10^{9} - 10^{10}	10^{9} - 10^{10}	1 - 2.5	SPT-20M [29]
BHC-1500	0.95 - 1	10^{12}	10^{12}	1 - 15	BHT-200 [30]
1.5 cm LaB6 Cathode	15 - 25	10^{12} - 10^{15}	10^{12} - 10^{15}	—	SPT Thrusters [31]
High Current LaB6	10 - 100	10^{11} - 10^{15}	10^{11} - 10^{15}	1 - 2	10 to 50 kW Thrusters [32]
HCA	50 - 100	—	—	1 - 6	NASA-300MS [33]

The electron current of the scandate cathode exceeds the electron current produced by the BHC-2500, SHC-M1, and the BHC-1500. The other three hollow cathodes are high power cathodes so it is expected that their electron current ranges would exceed that of the planar scandate cathode. The electron density and plasma density produced by the planar scandate cathode is on the order of 10^{13} cm^{-3} which falls in the middle of the electron and plasma densities ranging from 10^{9} cm^{-3} to 10^{15} cm^{-3} as presented in Table 2. Finally, the electron temperature produced by the scandate

cathode is comparable to the electron temperatures produced by the cathodes that successfully operate Hall thrusters. Since the measured plasma properties for the planar scandate cathode are similar in magnitude to the others presented here, it is reasonable to assume that the planar scandate cathode is a candidate for operation of a Hall thruster.

In addition to the plasma property criteria, the cathode must be able to supply the electron current required to operate a Hall thruster. The planar scandate cathode has demonstrated up to 3 A of electron current therefore it is likely to operate Hall thrusters that require up to 3 A of discharge current. A list of thrusters that are potential candidates for operation with the planar scandate cathode is shown in Table 3.

Table 3 Possible thrusters [34–38]

Thruster	Power (W)	Voltage (V)	Current (A)
SPT-70	95	43.2	2.2
BHT-100	100	200	0.2
BHT-200	200	250	0.8
SPT-50	220	180	1.2
SPT-50M	220	300	1
R-200	250	275	0.9
ST40	450	300	1.5
BHT-600	600	300	2
JPL MaSMi	1000	500	2

The Hall thrusters listed in Table 3 range in power levels from 95 W to 1 kW. Based on the discharge current required, the planar scandate cathode is likely to be capable of operating Hall thrusters across a wide range of power levels. Based on this analysis, it is reasonable to conclude that the planar scandate cathode is a candidate to operate a Hall thruster.

IV. Conclusion

In this study the e beam, inc. planar scandate cathode was evaluated to determine the feasibility of the cathode to produce electron current and plasma properties relevant to Hall effect thruster operation. The cathode was evaluated in cup connected mode as well as cup disconnected mode over a range of heater temperatures and anode currents to observe the cathode's operational characteristics. Further analysis was conducted on the cup disconnected mode data and the electron current, electron current density, electron density, plasma density, and electron temperature of the plasma produced by the cathode was determined. The cathode produced a maximum electron current of 3 A, a maximum electron current density of 616 $\frac{A}{cm^2}$, an average electron density and plasma density on the order of 10^{13} cm^{-3}, and an electron temperature ranging from 0.53 eV to 0.87 eV. These plasma properties were compared with the plasma properties of existing cathodes that successfully operate Hall thrusters and were found to be comparable. It was shown that the planar scandate cathode can reliably produce 3 A of electron current (discharge current), suggesting it may be viable for operation with a range of Hall thrusters. Based on the measured plasma properties and the demonstrated discharge current, it is reasonable to conclude that the e beam, inc. planar scandate cathode is a candidate to support Hall thruster operation.

Funding Sources

This work was partially supported by NASA through the Joint Advanced Propulsion Institute, A NASA Space Technology Research Institute, grant number 80NSSC21K1118. This work was also partially supported by the National Defense Science and Engineering Graduate Fellowship program, fellowship number NDSEG9643AAENG.

References

[1] Goebel, D. M., and Katz, I., *Fundamentals of electric propulsion: ion and Hall thrusters*, Wiley, Hoboken, N.J., 2008. OCLC: 299047879.

[2] Georgin, M., "Ionization Instability of the Hollow Cathode Plume," Ph.D. Dissertation, University of Michigan, Ann Arbor, MI, 2020. URL http://deepblue.lib.umich.edu/handle/2027.42/155210.

[3] Polk, J., Mikellides, I., Capece, A., and Katz, I., "Barium Depletion in Hollow Cathode Emitters," *45th AIAA/ASME/SAE/ASEE Joint Propulsion Conference & Exhibit*, American Institute of Aeronautics and Astronautics, Denver, Colorado, 2009, pp. 1–12. https://doi.org/10.2514/6.2009-5197.

[4] Mishra, K. C., Garner, R., and Schmidt, P. C., "Model of work function of tungsten cathodes with barium oxide coating," *Journal of Applied Physics*, Vol. 95, No. 6, 2004, pp. 3069–3074. https://doi.org/10.1063/1.1646451.

[5] Tighe, W., "Hollow Cathode Life Issues," *2006 IEEE International Vacuum Electronics Conference held Jointly with 2006 IEEE International Vacuum Electron Sources*, 2006, pp. 319–320. https://doi.org/10.1109/IVELEC.2006.1666312.

[6] Liu, X., Zhou, Q., Maxwell, T. L., Vancil, B. K., Beck, M. J., and Balk, T. J., "Scandate cathode surface characterization: Emission testing, elemental analysis and morphological evaluation," *Materials Characterization*, Vol. 148, 2019, pp. 188–200. https://doi.org/10.1016/J.MATCHAR.2018.12.013.

[7] Polk, J., "The Effect of Reactive Gases on Hollow Cathode Operation," *42nd AIAA/ASME/SAE/ASEE Joint Propulsion Conference & Exhibit*, American Institute of Aeronautics and Astronautics, Sacramento, California, 2006, pp. 1–20. https://doi.org/10.2514/6.2006-5153.

[8] Guerrero Vela, P. P., "Plasma Surface Interactions in LaB6 Hollow Cathodes with Internal Xe Gas Discharge," Ph.D. Dissertation, California Institute of Technology, Pasadena, CA, 2019. https://doi.org/10.7907/4CW7-2K35.

[9] Goebel, D. M., Watkins, R. M., and Jameson, K. K., "LaB 6 Hollow Cathodes for Ion and Hall Thrusters," *Journal of Propulsion and Power*, Vol. 23, 2007. https://doi.org/10.2514/1.25475.

[10] Becatti, G., and Goebel, D. M., "500-A LaB6 Hollow cathode for high power electric thrusters," *Vacuum*, Vol. 198, 2022. https://doi.org/10.1016/J.VACUUM.2022.110895.

[11] Gibson, J., Haas, G., and Thomas, R., "Investigation of scandate cathodes: emission, fabrication, and activation processes," *IEEE Transactions on Electron Devices*, Vol. 36, No. 1, 1989, pp. 209–214. https://doi.org/10.1109/16.21207.

[12] Kirkwood, D. M., Gross, S. J., Balk, T. J., Beck, M. J., Booske, J., Busbaher, D., Jacobs, R., Kordesch, M. E., Mitsdarffer, B., Morgan, D., Palmer, W. D., Vancil, B., and Yater, J. E., "Frontiers in Thermionic Cathode Research," *IEEE TRANSACTIONS ON ELECTRON DEVICES*, Vol. 65, 2018. https://doi.org/10.1109/TED.2018.2804484.

[13] Vancil, B., Jones, D., Ohlinger, W., Green, M., Kleschuk, M., and Schmidt, V., "Recent Progress on Scandate Cathodes," *2020 IEEE 21st International Conference on Vacuum Electronics (IVEC)*, 2020. https://doi.org/10.1109/IVEC45766.2020.9520643.

[14] Vancil, B., Lorr, J., Schmidt, V., Vancil, A., and Ohlinger, W., "Scandate cathode performance comparisons," *2016 IEEE International Vacuum Electronics Conference (IVEC)*, 2016. https://doi.org/10.1109/IVEC.2016.7561808.

[15] Ohlinger, W. L., Vancil, B., and Polk, J. E., "Advanced Dispenser-Type Cathode Development for Electric Propulsion," *52nd AIAA/SAE/ASEE Joint Propulsion Conference*, American Institute of Aeronautics and Astronautics, 2016, pp. 1–9. https://doi.org/10.2514/6.2016-4733.

[16] Ohlinger, W. L., Vancil, B., Polk, J. E., Schmidt, V., and Lorr, J., "Hollow Cathodes for Electric Propulsion Utilizing Scandate Cathodes," *51st AIAA/SAE/ASEE Joint Propulsion Conference*, American Institute of Aeronautics and Astronautics, 2015, pp. 1–7. https://doi.org/10.2514/6.2015-4009.

[17] Vancil, B., Schmidt, V., Lorr, J., and Brodie, I., "Scandate cathode with sharp transition," *2013 IEEE 14th International Vacuum Electronics Conference (IVEC)*, IEEE, Paris, France, 2013, pp. 1–2. https://doi.org/10.1109/IVEC.2013.6571037.

[18] Vancil, B., Lorr, J., Schmidt, V., Vancil, A., and Ohlinger, W., "Scandate cathode performance comparisons," *2016 IEEE International Vacuum Electronics Conference (IVEC)*, 2016, pp. 1–2. https://doi.org/10.1109/IVEC.2016.7561808.

[19] Vancil, B., Jones, D., Kleschuk, M., Schmidt, V., Vancil, A., Ohlinger, W., and Green, M., "Recent Progress on Scandate Cathodes," *2020 IEEE 21st International Conference on Vacuum Electronics (IVEC)*, 2020, pp. 81–82. https://doi.org/10.1109/IVEC45766.2020.9520643.

[20] Brodie, I., and Vancil, B., "The nature of the emitting surface of scandate cathodes," *IEEE International Vacuum Electronics Conference*, 2014, pp. 53–54. https://doi.org/10.1109/IVEC.2014.6857486.

[21] Ohlinger, W. L., "Low-Power Hollow Cathode for Smallsat/Cubesat Electric Propulsion Applications," *AIAA Propulsion and Energy 2021 Forum*, American Institute of Aeronautics and Astronautics, 2021, pp. 1–4. https://doi.org/10.2514/6.2021-3386.

[22] Vancil, B. K., Kowalski, J., and Shaver, J., "Micro-thruster cathode assembly," *United States Patent and Trademark Office*, Patent No.: US10794371B2, 2020, pp. 1–10. URL https://patents.google.com/patent/US10794371B2/en?oq=10794371.

[23] Polzin, K. A., Blumhagen, E., Sherrod, A. C., and Moeller, T., "Behavior of Triple Langmuir Probes in Non-equilibrium Plasmas," *AIAA Propulsion and Energy 2019 Forum*, American Institute of Aeronautics and Astronautics, Indianapolis, IN, 2019, pp. 1–12. https://doi.org/10.2514/6.2019-3990.

[24] Huddlestone, R. H., and Leonard, S. L. (eds.), *Plasma diagnostic techniques*, No. 21 in Pure and applied physics, Acad. Press, New York, NY, 1965.

[25] Hutchinson, I. H., *Principles of plasma diagnostics*, second edition ed., Cambridge University Press, Cambridge, 2005.

[26] Chen, F. F., "Lecture Notes on Langmuir Probe Diagnostics," *IEEE-ICOPS meeting: Mini-Course on Plasma Diagnostics*, Jeju, Korea, 2003, pp. 1–42. URL https://www.seas.ucla.edu/~ffchen/Publs/Chen210R.pdf.

[27] Lev, D. R., Mikellides, I. G., Pedrini, D., Goebel, D. M., Jorns, B. A., and McDonald, M. S., "Recent progress in research and development of hollow cathodes for electric propulsion," *Reviews of Modern Plasma Physics*, Vol. 3, No. 1, 2019, p. 6. https://doi.org/10.1007/s41614-019-0026-0.

[28] Taillefer, Z. R., Blandino, J. J., and Szabo, J., "Characterization of a Barium Oxide Cathode Operating on Xenon and Iodine Propellants," *Journal of Propulsion and Power*, Vol. 36, No. 4, 2020, pp. 575–585. https://doi.org/10.2514/1.B37315.

[29] Vekselman, V., Krasik, Y. E., Gleizer, S., Gurovich, V. T., Warshavsky, A., and Rabinovich, L., "Characterization of a Heaterless Hollow Cathode," *Journal of Propulsion and Power*, Vol. 29, No. 2, 2013, pp. 475–486. https://doi.org/10.2514/1.B34628.

[30] Asselin, D. J., "Characterization of the Near-Plume Region of a Low-Current Hollow Cathode," Master's Thesis, Worchester Polytechnic Institute, Worchester, Massachusetts, Apr. 2011.

[31] Becatti, G., Goebel, D. M., Polk, J. E., and Guerrero, P., "Life Evaluation of a Lanthanum Hexaboride Hollow Cathode for High-Power Hall Thruster," *Journal of Propulsion and Power*, Vol. 34, No. 4, 2018, pp. 893–900. https://doi.org/10.2514/1.B36659.

[32] Chu, E., and Goebel, D. M., "High-Current Lanthanum Hexaboride Hollow Cathode for 10-to-50-kW Hall Thrusters," *IEEE Transactions on Plasma Science*, Vol. 40, No. 9, 2012, pp. 2133–2144. https://doi.org/10.1109/TPS.2012.2206832.

[33] Thomas, R. E., Kamhawi, H., and Williams, G. J., "High Current Hollow Cathode Plasma Plume Measurements," *33rd International Electric Propulsion Conference*, Washington DC, 2013, pp. 1–17. URL https://ntrs.nasa.gov/citations/20140010692.

[34] Szabo, J. J., Tedrake, R., Metivier, E., Paintal, S., and Taillefer, Z., "Characterization of a One Hundred Watt, Long Lifetime Hall Effect Thruster for Small Spacecraft," *53rd AIAA/SAE/ASEE Joint Propulsion Conference*, American Institute of Aeronautics and Astronautics, Atlanta, GA, 2017, pp. 1–15. https://doi.org/10.2514/6.2017-4728.

[35] Conversano, R. W., Lobbia, R. B., Kerber, T. V., Tilley, K. C., Goebel, D. M., and Reilly, S. W., "Performance characterization of a low-power magnetically shielded Hall thruster with an internally-mounted hollow cathode," *Plasma Sources Science and Technology*, Vol. 28, No. 10, 2019, p. 105011. https://doi.org/10.1088/1361-6595/ab47de.

[36] Ekholm, J., Hargus, W., Larson, C., Nakles, M., Reed, G., and Niemela, C., "Plume Characteristics of the Busek 600 W Hall Thruster," *42nd AIAA/ASME/SAE/ASEE Joint Propulsion Conference & Exhibit*, Joint Propulsion Conferences, American Institute of Aeronautics and Astronautics, 2006, pp. 1–10. https://doi.org/10.2514/6.2006-4659.

[37] Szabo, J., Gray, S., Sheehan, F., Hinckley, J., Sawyer, S., Costa, W., Yu, T., and Taillefer, Z., "High Speed Plasma Probe and Electronics Suite," *37th International Electric Propulsion Conference*, Electric Rocket Propulsion Society, 2022, pp. 1–24.

[38] NASA, "State-of-the-Art of Small Spacecraft Technology - NASA," Tech. Rep. TP–2020-5008734, Small Spacecraft Systems Virtual Institute, 2020. URL https://www.nasa.gov/smallsat-institute/sst-soa/.